

© © 2015 IEEE. Personal use of this material is permitted. Permission from IEEE must be obtained for all other uses, in any current or future media, including reprinting/republishing this material for advertising or promotional purposes, creating new collective works, for resale or redistribution to servers or lists, or reuse of any copyrighted component of this work in other works.

Title: Sequential Spectral Change Vector Analysis for Iteratively Discovering and Detecting

Multiple Changes in Hyperspectral Images

This paper appears in: IEEE Transactions on Geoscience and Remote Sensing

Date of Publication: 27 February 2015

Author(s): S. Liu, L. Bruzzone, F. Bovolo, M. Zanetti, P. Du

Volume: 53, Issue: 8

Page(s): 4363 - 4378

DOI: 10.1109/TGRS.2015.2396686

# SEQUENTIAL SPECTRAL CHANGE VECTOR ANALYSIS FOR ITERATIVELY DISCOVERING AND DETECTING MULTIPLE CHANGES IN HYPERSPECTRAL IMAGES

Sicong Liu, *Student Member, IEEE*, Lorenzo Bruzzone, *Fellow, IEEE*, Francesca Bovolo, *Senior Member, IEEE*, Massimo Zanetti, and Peijun Du, *Senior Member, IEEE*  
e-mail: [bruzzone@ing.unitn.it](mailto:bruzzone@ing.unitn.it)

## ABSTRACT

This paper presents an effective semi-automatic method for discovering and detecting multiple changes (i.e., different kinds of changes) in multitemporal hyperspectral images. Differently from the state-of-the-art techniques, the proposed method is designed to be sensitive to the small spectral variations that can be identified in hyperspectral (HS) images but usually are not detectable in multispectral (MS) images. The method is based on the proposed Sequential Spectral Change Vector Analysis ( $S^2CVA$ ), which exploits an iterative hierarchical scheme that at each iteration discovers and identifies a subset of changes. The approach is interactive and semi-automatic and allows one to study in detail the structure of changes hidden in the variations of the spectral signatures according to a top-down procedure. A novel 2-D Adaptive Spectral Change Vector Representation (ASCVR) is proposed to visualize the changes. At each level this representation is optimized by an automatic definition of a reference vector that emphasizes the discrimination of changes. Finally, an interactive manual change identification is applied for extracting changes in the ASCVR domain. The proposed approach has been tested on three hyperspectral data sets including both simulated and real multitemporal images showing multiple-change detection problems. Experimental results confirmed the effectiveness of the proposed method.

## Keywords

Change detection; change visualization; change representation; multiple changes; change vector analysis (CVA); hyperspectral images; multi-temporal images; remote sensing.

## I. INTRODUCTION

For decades, Earth Observation (EO) satellites have provided a unique way to observe our living planet from space. Thanks to the revisit property of EO satellites, a huge amount of multitemporal images is now available in archives. This allows us to monitor the land surface changes in wide geographical areas according to both long term (e.g., yearly) and short term (e.g., daily) observations. The detection and understanding of changes occurred in the multitemporal images is essential for studying the global change, the environmental evolution and the anthropic phenomena [1]. Change Detection (CD) is the process designed to identify changes occurred on the same geographical area at different observation times [1], [2]. CD techniques have been widely and successfully used in several remote sensing applications (e.g., environmental monitoring, agriculture, disaster monitoring) in the past decades, especially considering multitemporal MS images [2], [3], [4], [5].

CD methods can be divided into two categories based on the final application purpose: i) binary change detection methods [6], [7], [8], [9], [10], [11], [12]; and ii) multiple change detection methods. Binary CD methods consider all kinds of changes as one single change class, thus their aim is to find the changed and no-changed pixels in the considered feature space ignoring the semantic meaning of the possible different kinds of changes. In the past decades, exhaustive investigations on this topic have been conducted on MS images, e.g., by considering manual thresholding [6], [7], automatic modeling and thresholding techniques [8], clustering [9], and other specific approaches [10], [11], [12]. In contrast to binary CD, the detection of multiple-change classes is a more challenging task. Some methods have been proposed in the literature to address this problem. If ground truth data are available, the most popular method is the supervised Post-Classification Comparison (PCC) [4]. Other approaches based on the multi-date classification [13], the compound classification [14] and the active learning based compound classification [15] were also successfully investigated. However, in real application scenarios, the ground truth data are usually not available. Therefore, unsupervised CD approaches that do not rely

on any reference sample are more attractive. Transformation-based techniques like Iteratively Reweighted Multivariate Alteration Detection (IR-MAD) [16], Temporal-Principal Components Analysis (T-PCA) [17], etc., were proposed and proven to be effective. We recall the Compressed Change Vector Analysis ( $C^2VA$ ) approach recently presented in the literature [18], which was developed based on the polar Change Vector Analysis (CVA) [19], [20]. Unlike CVA, the  $C^2VA$  allows a visualization and detection of multiple changes by considering all the available spectral channels within a 2-D representation. Thus  $C^2VA$  method theoretically allows one to detect all possible change classes occurred between the considered images, without neglecting any spectral band or working on their selection. Despite the  $C^2VA$  representation exploits a lossy compression of the information, it has proven to be successful in addressing multiple-change detection problems in MS images [18], [21].

The growing availability of HS data brings the remote sensing into a high spectral resolution era. HS sensors take images having a very high spectral resolution (e.g., 10nm) over a wide spectral range (e.g., 400nm-2500nm). In change detection, this important property allows one to potentially detect small spectral variations that are usually not detectable in MS images due to the poor spectral representation (i.e., generally sufficient for representing only the major abrupt changes) [22]. Accordingly, robust CD techniques should be developed to take full advantage of the rich spectral information contained in HS data, and to effectively identify the multiple-change information. In this paper we focus on the problem of representation and analysis of multiple change information in HS images.

Despite the successful definition of a large number of effective CD techniques for MS images, these techniques reduce their efficiency when HS images are considered mainly due to: 1) the high-dimensionality of the feature space; 2) the presence of noisy channels and redundant information; 3) the increase of computational cost; 4) the increase of the possible number of changes; and 5) the high complexity of the change representation and identification process. In particular, the last two items may strongly affect the effectiveness of CD methods, like the  $C^2VA$ , because it might be highly difficult (in

some cases impossible) to: i) identify successfully all the existing change clusters and thus the correct number of changes; and ii) model and extract each single change class. Therefore, more advanced and sophisticated approaches should be designed to properly handle the challenging issues in multitemporal HS images. Recently, we proposed an unsupervised hierarchical spectral change vector analysis (HSCVA) method that addresses the considered problem via a hierarchical clustering procedure [23]. At each level of the processing, automatic clustering is applied based on the principal components to estimate the number of changes and to discriminate them in different clusters. Although the usefulness of HSCVA has been proven in real hyperspectral CD cases, HSCVA does not allow an explicit, detailed and interactive analysis of the changes in the spectral signatures of multitemporal images.

In this paper, the multiple-change detection problem in HS images (CD-HS) is analyzed from the spectral signature point of view. The limitations that result in the degradation of performance when  $C^2VA$  is applied to HS images are studied. A novel Sequential Spectral Change Vector Analysis ( $S^2CVA$ ) approach is proposed, which: 1) discovers and analyzes the multiple changes at different spectral levels through a top-down hierarchical architecture; 2) at each level provides a visualization of multiple changes in a 2-D representation domain; 3) is designed in a sequential, interactive and semi-automatic fashion. In detail, the proposed approach addresses the CD problem as follows. First, a binary CD step is applied to HS multitemporal images to extract in a conservative way the changed pixels from the whole difference image. Then the attention is focused only on the changed pixels, and a novel adaptive 2-D change representation (ASCVR) is proposed to visualize the possible different changes. Changes are separated between each other according to an interactive change identification scheme. Then the process moves to the next level and iterates on each of the identified changes until convergence is reached. Finally, the change-detection map is generated by merging the detected change classes derived at each level of the hierarchy. Note that at each step of the hierarchical processing, the proposed technique emphasizes a specific portion of the change information in the whole Spectral Change Vector

(SCV) feature space. This is accomplished by adaptively generating proper change variables for the 2-D change representation. The proposed  $S^2CVA$  approach is validated on three data sets including: 1) simulated bi-temporal images based on an AVIRIS hyperspectral image; 2) real bi-temporal hyperspectral images acquired by the Hyperion sensor onboard of Earth Observing-1 (EO-1) satellite; and 3) simulated bi-temporal images based on a hyperspectral camera image. Experimental results confirm the effectiveness of the proposed method for addressing the multiple-change detection problem in multitemporal HS images.

The rest of the paper is organized as follows. Section II reviews the  $C^2VA$  approach and discusses some important issues and challenges when transferring the CD perspective from MS to HS cases. The proposed sequential CD technique (i.e.,  $S^2CVA$ ) is described in Section III. Section IV introduces the used HS data, reports and analyzes the obtained experimental results. Finally, Section V draws the conclusion of this work.

## II. MULTIPLE-CHANGE DETECTION BY $C^2VA$ IN MULTI/HYPER-SPECTRAL IMAGES

Let us first formalize the multiple-change detection problem for multi/hyper-spectral images. Let  $X_1$  and  $X_2$  be two co-registered multi/hyper-spectral images acquired over the same geographical area at times  $t_1$  and  $t_2$ , respectively. The multitemporal difference image  $X_D$  (and thus the SCVs associated with each pixel) is computed by subtracting the two images pixel by pixel, i.e.,

$$X_D = X_2 - X_1 \quad (1)$$

Let  $\Omega = \{\omega_n, \Omega_c\}$  be the set of all classes in  $X_D$ , where  $\omega_n$  is the no-change class and  $\Omega_c = \{\omega_{c_1}, \omega_{c_2}, \dots, \omega_{c_k}\}$  is the set of the  $K$  possible change classes. The considered CD problem can be defined as to detect all changed pixels ( $\Omega_c$ ) and to separate them into multiple change classes  $\{\omega_{c_1}, \omega_{c_2}, \dots, \omega_{c_k}\}$ .

### A. The standard $C^2VA$

In the standard  $C^2VA$  method, a compressed change representation in a 2-D polar domain is defined by two change variables, i.e. the magnitude  $\rho$  and the direction  $\alpha$  [18]:

$$\rho = \sqrt{\sum_{b=1}^B (X_D^b)^2} \quad (2)$$

$$\alpha = \arccos \left[ \frac{1}{\sqrt{B}} \left( \sum_{b=1}^B X_D^b / \sqrt{\sum_{b=1}^B (X_D^b)^2} \right) \right] \quad (3)$$

where  $X_D^b$  is the  $b$ -th ( $b=1, \dots, B$ ) component of  $X_D$  and  $B$  is the number of spectral channels of the considered images (i.e., the dimensionality of SCVs). The magnitude  $\rho$  is defined based on the popular Euclidean distance [22]. It measures the total contribution of spectral change brightness, whereas it is not sensitive to the shape of spectral vectors. The angle distance  $\alpha$  is measured by the Spectral Angle Distance (SAD) [24], which is widely used in several hyperspectral application fields for material identification, classification, etc. [24], [25], [26]. SAD measures the similarity between two given spectral signatures, especially focusing on the shape of the spectrum.

Variables  $\rho$  and  $\alpha$  define a 2-D polar coordinate domain  $\mathbf{D}$  [18] as:

$$\mathbf{D} = \{ \rho \in [0, \rho_{\max}] \text{ and } \alpha \in [0, \pi] \} \quad (4)$$

where  $\rho_{\max}$  is the maximum value of  $\rho$ . All the SCVs in  $X_D$  can be represented in a 2-D semicircle scattergram (see Fig.1). This scattergram allows one to easily visualize multidimensional change information in a 2-D feature space. However, the compression from a  $B$ -D space into a 2-D space results in a loss of information and thus in ambiguity on the detection of different kinds of changes.

In the  $C^2VA$  framework, the multiple-change detection problem is addressed according to two steps [18]:

- 1) Set threshold  $T_\rho$  along  $\rho$  variable to divide the whole semicircle of the  $C^2VA$  representation domain into two parts, i.e.,  $SC_n$  and  $SA_c$  (see Fig.1), which are related to the unchanged ( $\omega_n$ ) and changed ( $\Omega_c$ ) SCVs, respectively:

$$SC_n = \{\rho, \alpha | 0 \leq \rho < T_\rho \text{ and } 0 \leq \alpha \leq \pi\} \quad (5)$$

$$SA_c = \{\rho, \alpha | T_\rho \leq \rho \leq \rho_{\max} \text{ and } 0 \leq \alpha \leq \pi\} \quad (6)$$

2) Separate multiple-change classes ( $\omega_{C_1}, \dots, \omega_{C_k}$ ) along the direction  $\alpha$  by analyzing the semiannulus  $SA_c$ .

Multiple angular thresholds  $T_{\alpha,k}$  ( $k=1, \dots, K-1$ ) can be defined to find  $K$  annular sectors (each corresponding to a change) inside  $SA_c$ :

$$S_k = \{\rho, \alpha | T_\rho \leq \rho < \rho_{\max} \text{ and } T_{\alpha,k} \leq \alpha \leq T_{\alpha,k+1}\} \quad (7)$$

where  $0 \leq T_{\alpha,k} < T_{\alpha,k+1} \leq \pi$ .

Note that thresholds  $T_\rho$  and  $T_\alpha$  can be detected manually or automatically according to one of the various methods proposed in the literature [8], [14], [27], [28].

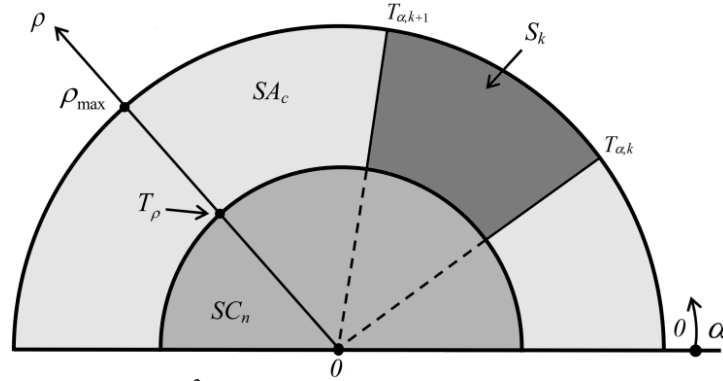


Fig.1 Compressed Change Vector Analysis (C<sup>2</sup>VA) for representing multiple-changes in the 2-D polar domain [18].

### B. Problems and challenges when applying C<sup>2</sup>VA to CD-HS cases

C<sup>2</sup>VA has proven to be effective when dealing with the MS images [1], [18], [21]. Due to the rough spectral resolution of MS images, the direction variable  $\alpha$  is generally effective to represent the relatively few abrupt changes that are visible in MS data and does not suffer too much of the loss of information associated with the compressed representation. However, in the CD-HS case the finer spectral resolution results in a high number of changes that can be detected [23]. Thus the compressed

representation of many spectral channels in one variable  $\alpha$  leads to a high probability of ambiguous description of changes, which may result in highly overlapped clusters in the  $C^2VA$  representation.

In multitemporal HS images, we can distinguish between two kinds of hierarchically related changes [23]: 1) major changes, which have a significant spectral difference with respect to both the no-change class and the other change classes; 2) subtle changes, whose SCVs are similar to those of an associated major change, but statistically significantly differ from each other in some portions of the spectrum. When subtle changes inside a major change are present, due to a high similarity among their SCVs, the  $\alpha$  variable defined on the basis of a fixed unit reference vector  $\mathbf{R} = [1/\sqrt{B}, \dots, 1/\sqrt{B}]$  (as the one derived in (3), [18]) is likely to be ineffective for their discrimination. To overcome this drawback, a robust definition to the reference vector  $\mathbf{R}$  (and thus the change variable  $\alpha$ ) should be designed. This definition should optimize the separation of changes and provide a meaningful change visualization in a hierarchical and adaptive way, thus to properly represent and discover as many changes present in the HS images as possible.

Accordingly, let us recall that the angle distance  $\alpha$  between SCVs in  $\mathbf{X}_D$  and a generic reference vector  $\mathbf{R}$  is defined as:

$$\alpha = \arccos \left[ \left( \frac{\sum_{b=1}^B (\mathbf{X}_D^b R^b)}{\sqrt{\sum_{b=1}^B (\mathbf{X}_D^b)^2 \sum_{b=1}^B (R^b)^2}} \right) \right], \quad \alpha \in [0, \pi] \quad (8)$$

where  $R^b$  is the  $b$ -th component of the reference vector  $\mathbf{R}$ . Due to the fact that  $\alpha$  is invariant to the multiplicative scaling [24], the reference  $\mathbf{R}$  in (8) actually can be extended to any constant vector  $\mathbf{R} = [a, \dots, a]$ , where  $a > 0$  and  $a \in \mathfrak{R}$ .

### III. PROPOSED SEQUENTIAL SPECTRAL CHANGE VECTOR ANALYSIS ( $S^2CVA$ )

Inspired by the aforementioned analysis and discussion on  $C^2VA$ , we are motivated to find a reliable solution to the problem of discovering, representing and discriminating different spectral changes in HS

images. The idea is to start from the  $C^2VA$  developed for MS images, and to overcome its drawbacks when applied to HS images. To this end, a novel Sequential Spectral Change Vector Analysis ( $S^2CVA$ ) is proposed. Differently from the standard  $C^2VA$ , the proposed  $S^2CVA$  is designed to be sensitive to the small changes in spectral signature behaviors, which are usually not detectable in MS images. Instead of having just a one shot processing as in the standard  $C^2VA$  (due to the measurement based on the fixed reference vector), the proposed  $S^2CVA$  allows an adaptive definition of the reference vector. The whole  $S^2CVA$  framework is designed in an iterative fashion. A novel unsupervised 2-D Adaptive Spectral Change Vector Representation (ASCVR) technique and a fast change identification scheme are designed aiming at better representing and discovering the possible multiple changes at each analysis level. This results in a sequence of 2-D representation scattergrams that can be obtained to model the multiple changes at different levels of the hierarchy taking into account the global and local spectral variations. Homogenous scattering clusters observed from a change representation scattergram at a given level are discriminated among each other and then are investigated individually in the next level. Note that the proposed  $S^2CVA$  is developed as a semi-automatic technique, which consists of: i) an adaptive change representation that permits to discover the multiple changes, and ii) a manual (interactive) change identification. The block scheme of the proposed CD approach is illustrated in Fig.2.

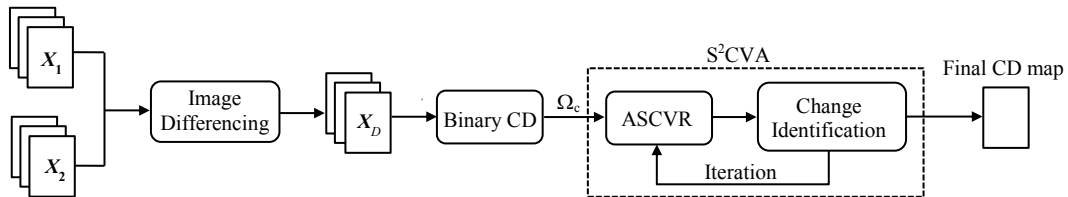


Fig.2 Block scheme of the proposed CD approach based on  $S^2CVA$ .

At the beginning, all SCVs in  $X_D$  belong to the same class  $\Omega$ . Once the binary CD result is obtained in level  $L_0$ , let  $P_0$  be the cluster representing SCVs associated with the general change cluster  $\Omega_c$  extracted

to initialize the whole sequential analysis. Note that in  $L_0$ , the binary CD is done as in the standard  $C^2VA$  method, where only the magnitude variable  $\rho$  is analyzed according to a proper thresholding technique (e.g., by using the EM algorithm in the framework of the Bayesian decision theory [8], [18]). In the next levels, let  $P_{i,j}$  be the  $j$ -th ( $j = 1, \dots, J_i$ ) change cluster observed at the  $i$ -th ( $i=1, \dots, I-1$ ) level  $L_i$  of the  $S^2CVA$  hierarchy, where  $J_i$  is the maximum number of change clusters at level  $i$ , and  $I$  is the total number of levels in the hierarchy. In the next subsections, firstly we define the ASCVR technique and then describe its use in the framework of the hierarchical analysis associated with the proposed  $S^2CVA$ .

#### *A. Proposed 2-D Adaptive Spectral Change Vector Representation (ASCVR)*

Similarly to  $C^2VA$ , the proposed ASCVR technique is designed in a 2-D feature space. The main reason for using a 2-D rather than a high dimensional (e.g.,  $B$ -D) feature space is that in this way it is easy to visualize the change clusters and their numbers. Instead of using a fixed reference vector  $\mathbf{R}$  as in  $C^2VA$  [18], the proposed ASCVR is designed to adaptively define the most suitable reference vector  $\mathbf{R}$  for analyzing the multiple changes at each considered hierarchical level. The selection of  $\mathbf{R}$  and the change representation are directly derived based on the statistic distribution of the input SCVs. Thus the proposed ASCVR is totally unsupervised.

The proposed ASCVR is defined by the change magnitude  $\rho$  (which is the same as defined in  $C^2VA$  (2)) and the compressed change direction  $\alpha$  (which represents the spectral angle distance between a given SCV in  $\mathbf{X}_D$  and a reference vector  $\mathbf{R}$  (8)). Different values of angle distance measure indicate different kinds of changes. At different levels of the proposed hierarchical analysis, for each specific portion of the SCV feature space associated with the considered change cluster, a new reference vector  $\mathbf{R}$  is defined. In greater details, the first eigenvector that corresponds to the maximum eigenvalue of the data covariance matrix of the SCVs associated to the considered cluster  $j$  at level  $i$  (i.e.,  $P_{i,j}$ ) is adopted as the reference vector. The selection of the first eigenvector is due to the fact that a 2-D change representation

is desired, which preserves as much as possible the spectral variations of the considered SCVs in a low-dimensional feature space that can be easily managed. In the proposed ASCVR, this vector shows a direction that maximizes the variance of the measurement on  $\alpha$ , thus resulting in an adaptive and effective representation of the hidden change patterns in the considered SCVs. For a considered generic cluster  $P_{i,j}$  in the hierarchy, the procedure for adaptively defining the reference vector  $\mathbf{R}_{i,j}$  is as follows.

Let us consider the covariance matrix  $\mathbf{A}_{i,j}$  of  $\mathbf{x}_{i,j}$  (denoted as the SCVs in  $P_{i,j}$ ):

$$\mathbf{A}_{i,j} = \text{cov}(\mathbf{x}_{i,j}) = E[(\mathbf{x}_{i,j} - E[\mathbf{x}_{i,j}])(\mathbf{x}_{i,j} - E[\mathbf{x}_{i,j}])^T] \quad (9)$$

where  $E[\mathbf{x}_{i,j}]$  is the expectation of  $\mathbf{x}_{i,j}$  and  $\mathbf{A}_{i,j}$  is the  $B \times B$  dimensional covariance matrix that represents  $\mathbf{x}_{i,j}$  by means of the eigenvectors and eigenvalues, which are calculated according to (10):

$$\mathbf{A}_{i,j} \cdot \mathbf{V}_{i,j} = \mathbf{V}_{i,j} \cdot \mathbf{W}_{i,j} \quad (10)$$

$\mathbf{W}_{i,j}$  is a diagonal matrix where the eigenvalues are sorted in descending order (i.e.,  $\lambda_{i,j}^1 > \lambda_{i,j}^2 > \dots > \lambda_{i,j}^B$ ) in the diagonal. The magnitude of eigenvalues reflects the amount of data variance that is captured by the corresponding eigenvectors. Let  $\mathbf{V}_{i,j} = [\mathbf{V}_{i,j}^1, \mathbf{V}_{i,j}^2, \dots, \mathbf{V}_{i,j}^B]$  be the matrix of eigenvectors. The reference vector  $\mathbf{R}_{i,j}$  for computing  $\alpha_{i,j}$  in (8) is selected as the first eigenvector  $\mathbf{V}_{i,j}^1$  that corresponds to the largest eigenvalue  $\lambda_{i,j}^1$ :

$$\mathbf{R}_{i,j} = \mathbf{V}_{i,j}^1 = \begin{pmatrix} v_1 \\ v_2 \\ \vdots \\ v_B \end{pmatrix}_{i,j} \quad (11)$$

Accordingly, the two change variables for the SCVs of the cluster  $P_{i,j}$  are defined as follows:

$$\begin{cases} \rho_{i,j} = \sqrt{\sum_{b=1}^B (\mathbf{x}_{i,j}^b)^2} \\ \alpha_{i,j} = \arccos \left[ \frac{\sum_{b=1}^B (\mathbf{x}_{i,j}^b R_{i,j}^b)}{\sqrt{\sum_{b=1}^B (\mathbf{x}_{i,j}^b)^2 \sum_{b=1}^B (R_{i,j}^b)^2}} \right] \end{cases} \quad (12)$$

The related 2-D representation domain  $\mathbf{D}_{i,j}$  is defined as:

$$\mathbf{D}_{i,j} = \{ \rho_{i,j} \in [0, \rho_{i,j}^{\max}] \text{ and } \alpha_{i,j} \in [0, \pi] \} \quad (13)$$

Note that the use of the first eigenvector does not guarantee the maximum discriminability in all cases, but this is an effective choice for an adaptive 2-D visualization of the latent change information.

### B. Proposed Sequential Spectral Change Vector Analysis ( $S^2CVA$ )

The intrinsic adaptive characteristic of the proposed ASCVR can be exploited to represent either the whole or a portion of the SCV space. Accordingly, the challenging CD-HS problem can be addressed hierarchically by the proposed Sequential Spectral Change Vector Analysis ( $S^2CVA$ ). The main idea is that a sequence of ASCVR scattergrams can be obtained for representing SCVs in different specific spectral levels, thus SCVs that are associated with different change classes can be gradually separated following the sequential analysis. The block scheme of the proposed  $S^2CVA$  method is shown in Fig.3.

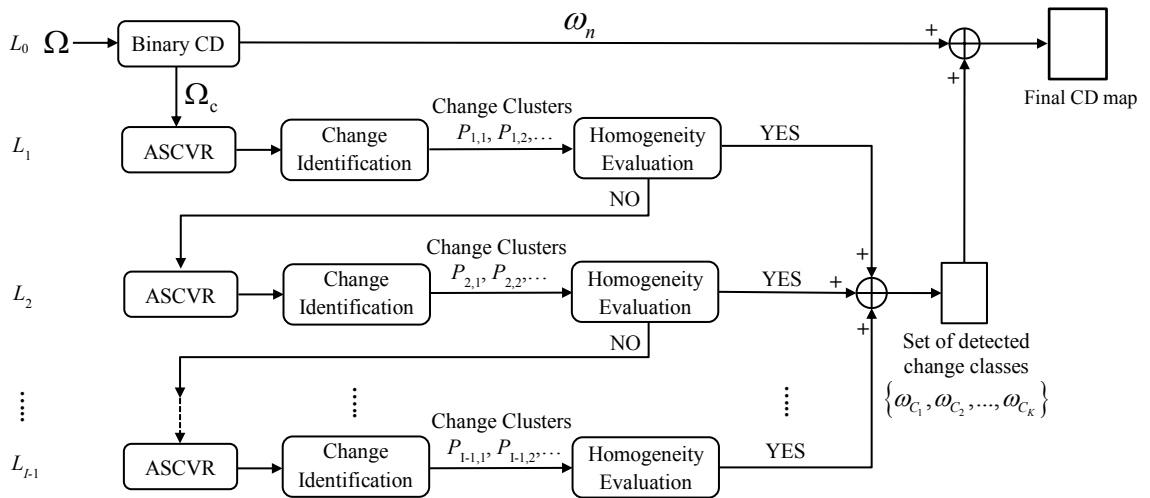


Fig.3 Block scheme of the proposed  $S^2CVA$  step.

The process begins at the initial level  $L_0$  of the hierarchy, where  $P_0$  is the initial change cluster obtained by thresholding the  $\rho$  variable. Then the sequential technique focuses on the  $P_0$  (i.e., SCVs that belong to  $\Omega_c$ ) in order to discover and identify the possible kinds of changes. At level  $L_1$ , if more than one homogenous clusters  $P_{1,1}, P_{1,2}, \dots, P_{1,J_1}$  is observed, changes need to be discriminated and separated among each other. Then the procedure moves to the next level  $L_2$ , focusing on each single cluster in  $\{P_{1,1}, P_{1,2}, \dots, P_{1,J_1}\}$  to continue the iterative change analysis by re-projecting the SCVs of each cluster in its corresponding new ASCVR domain. Thus this is to explore if more possible changes at this level of representation can be discovered. The ASCVR scheme defined in the Section III-A is used for each considered change cluster, thus the corresponding 2-D change representations  $D_{1,j}$  are built by automatically updating the references  $\mathbf{R}_{1,j}$  (and thus  $\alpha_{1,j}$ ) according to the SCVs  $\mathbf{x}_{1,j}$  in  $P_{1,j}$  ( $j=1, \dots, J_1$ ). By considering the intrinsic properties of SCVs that SCVs belong to a given change class have homogenous behaviors on the change variables, thus a single cluster are expected to be observed on their representation domain. On the contrary, different clusters that can be discriminated in the ASCVR scattergram indicate possible different kinds of changes. A manual procedure is applied interactively by the user. For each observed change cluster, a discrimination boundary is manually defined, which is structured as a polygon in the software prototype we implemented. Note that boundaries are selected independently for each observed change cluster. At a given level of S<sup>2</sup>CVA the homogeneity is evaluated manually. The convergence is reached when only a single homogenous change cluster is observed in the scattergram. The cluster is finally associated to a change class in  $\{\omega_{C_1}, \omega_{C_2}, \dots, \omega_{C_K}\}$  and the SCVs of that change class are reversely mapped into the image space to generate the CD map. The whole CD procedure is completed when each representation of the considered specific portion of SCVs in the hierarchy achieves convergence. The whole S<sup>2</sup>CVA hierarchy can be modeled as a tree-structure (see the example in Fig.4). The final multiple-change detection map is the union of all the detected

change classes  $\{\omega_{c_1}, \omega_{c_2}, \dots, \omega_{c_k}\}$  and the extracted no-change class  $\omega_h$  (i.e., the union of all the leaf nodes in the tree). It is worth noting that by following the proposed sequential analysis, the original global change representation and optimization problem is decomposed into several local sub-problems at different levels. Thus many potential changes can be detected hierarchically taking into account different levels of spectral change significance.

The proposed  $S^2CVA$  method allows the user to have effective interactions with the change representation and discovery (in the 2-D representation domain), and the change extraction (in the original image domain). At the end of the process the obtained hierarchical tree completely describes major and subtle changes present in the considered HS multitemporal images and their parental relations.

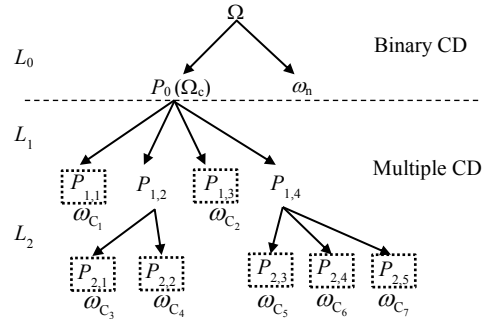


Fig.4 Example of the obtained three-level hierarchical tree by the proposed CD method based on  $S^2CVA$ , where seven of the leaf nodes are detected as change classes and one as the no-change class.

## IV. EXPERIMENTAL RESULTS

### A. Data Set 1: Simulated Hyperspectral Remote Sensing Data Set

The first data set is made up of a real single-time hyperspectral image acquired by the AVIRIS sensor in 1998 over Salinas Valley, California. This image was downloaded from the website of computational intelligence group from the Basque University (UPV/EHU) [29]. The original image contains 224 contiguous spectral bands with wavelength from 400nm to 2500nm. The image is characterized by a spatial resolution of 3.7m and a spectral resolution of 10nm and has a size of  $512 \times 217$  pixels. This data set was originally used for testing a HS image classification task with the available ground truth that has

16 classes mainly including vegetation, bare soil, and vineyard. In the pre-processing phase, 20 water absorption bands (i.e., bands 108-112, 154-167 and 224) were discarded thus obtaining 204 bands for our experiments. By taking advantage of the available ground truth data, we simulated and generated the changed image (considered as  $X_2$ ) based on the original image (considered as  $X_1$ ) according to the following steps: i) 15 tiles (i.e., regions) were extracted from the original image  $X_1$  (see Fig.5.a), which cover different land-cover classes. ii) The extracted tiles were inserted in different areas on  $X_1$  by replacing the spectral vectors over all bands. The same operation was done for all tiles to simulate an image ( $X_2$ ) with eight different change classes. iii) A small constant bias value was applied to  $X_2$  to simulate a stationary difference in light condition. iv) White Gaussian noise was added to  $X_2$  by setting an SNR equal to 10 dB. The reason for testing with the simulated data is that all the details can be quantitatively investigated in a controlled environment. False color composites of  $X_1$  and  $X_2$  are shown in Fig.5 (a) and (b), respectively. The reference map is reported in Fig.5 (c). Detailed class transitions are listed in TABLE I with the corresponding number of samples in each simulated change class.

The proposed  $S^2CVA$  approach was compared with other literature multiple change detection methods. First, the proposed  $S^2CVA$  and the standard  $C^2VA$  [18] representations were visually compared. Then change detection results were discussed through both a qualitative and a quantitative analysis based on the change reference map. The following techniques were considered for comparison: 1) standard automatic thresholding in the  $C^2VA$  feature space ( $C^2VA\_T$ ) [18]; 2) manual (interactive) change identification in the  $C^2VA$  feature space ( $C^2VA\_M$ ); 3)  $k$ -means clustering on the whole changed SCVs ( $k$ -means\_SCVs); 4) proposed  $S^2CVA$  approach using manual (interactive) change identification at each level of the representation ( $S^2CVA\_M$ ). For the  $k$ -means\_SCVs, the results are given as the average over 20 random initializations of the  $k$ -means algorithm. Note that advantages were given to the  $k$ -means clustering by fixing the number of clusters (i.e., changes) as being known a priori. EM algorithm was used in the framework of the Bayesian decision theory for estimating the thresholds in the  $C^2VA\_T$  [18].

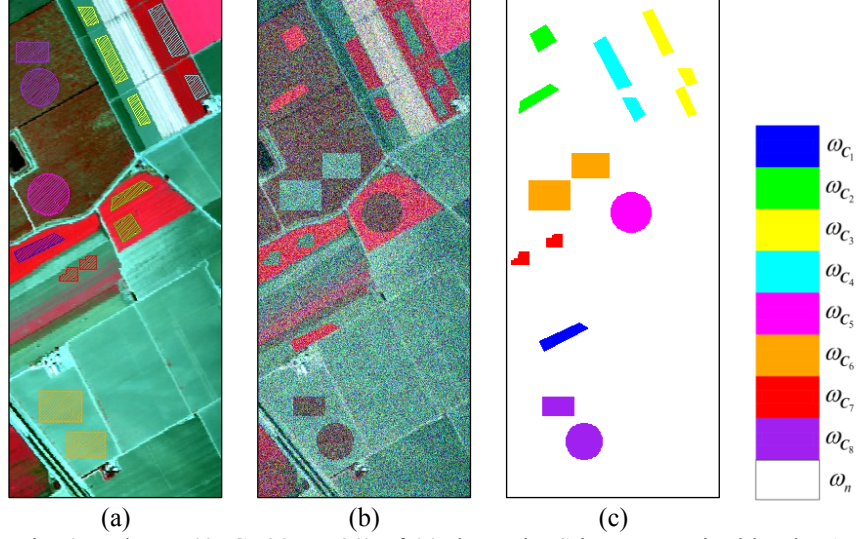


Fig.5 False color composite (Bands: R: 40, G: 30, B: 20) of (a) the real HS image acquired by the AVIRIS sensor in Salinas scenario ( $X_1$ ) and (b) the simulated changed image ( $X_2$ ) computed with an additive white Gaussian noise; (c) the change reference map (eight changes in different colors, and no-change class in white color).

**TABLE I**  
**SIMULATED CHANGES IN SALINAS DATA SET AND THE CORRESPONDING NUMBER OF SAMPLES**

| Change class   | Simulated changes (from $X_1$ to $X_2$ )                      | Samples (Number of pixels) |
|----------------|---|----------------------------|
| $\omega_{C_1}$ | Brocoli_green_weeds_1 $\rightarrow$ Corn_senesced_green_weeds | 534                        |
| $\omega_{C_2}$ | Brocoli_green_weeds_2 $\rightarrow$ Vinyard_untrained         | 878                        |
| $\omega_{C_3}$ | Fallow_smooth $\rightarrow$ Celery                            | 1149                       |
| $\omega_{C_4}$ | Celery $\rightarrow$ Fallow_smooth                            | 1163                       |
| $\omega_{C_5}$ | Grapes_untrained $\rightarrow$ Brocoli_green_weeds_2          | 1402                       |
| $\omega_{C_6}$ | Soil_vinyard_develop $\rightarrow$ Grapes_untrained           | 2347                       |
| $\omega_{C_7}$ | Lettuce_romaine_5wk $\rightarrow$ Brocoli_green_weeds_1       | 420                        |
| $\omega_{C_8}$ | Vinyard_untrained $\rightarrow$ Soil_vinyard_develop          | 1812                       |
| $\omega_n$     | No-change   | 101399                     |

Fig.6 (a) shows the scattergram of all SCVs in the standard  $C^2VA$  feature space. In the binary CD step, threshold  $T_\rho$  was automatically estimated and resulted equal to 1.929 (see the red semicircle in Fig.6.a). Six change clusters can be observed from the  $C^2VA$  representation (despite eight were expected). The manual discrimination boundaries based on polygons were defined to separate them among each other and to extract the SCVs that correspond to each single cluster (see Fig.6.a, where the discrimination boundaries are defined in yellow polygons). From a comparison with the reference map, it was found

that the correspondences among the six detected change clusters and the eight reference change classes are:  $\omega_{C_6}$ ,  $\omega_{C_2}$ ,  $\omega_{C_1} \cup \omega_{C_7}$ ,  $\omega_{C_3} \cup \omega_{C_4}$ ,  $\omega_{C_5}$  and  $\omega_{C_8}$ . Therefore, two clusters include different classes in the  $C^2VA$  representation. Moreover, some overlapped clusters (e.g., area between  $\omega_{C_2}$  and  $\omega_{C_6}$ , and the one between  $\omega_{C_5}$  and  $\omega_{C_8}$  in Fig.6.a) in the  $C^2VA$  representation cause detection errors, thus reducing the overall accuracy. If we separate the clusters with the discrimination boundaries reported in Fig.6 (a), the obtained CD map is shown in Fig.8 (b), where the detected six changes appear in different colors.

The same CD-HS task was addressed by using the proposed  $S^2CVA\_M$  approach. We implemented it starting from the initial input  $\Omega$  in  $L_0$ . The same threshold  $T_\rho$  estimated for  $C^2VA$  was used to separate  $\Omega_c$  and  $\omega_n$  (see the red semicircle in Fig.6.b). Six clusters inside of the general  $\Omega_c$  class ( $P_0$ ) were manually identified and separated into  $P_{1,1}, \dots, P_{1,6}$  according to the defined discrimination boundaries in Fig.6 (b). Then the processing moved into the next level (i.e.,  $L_1$ ) and focused on each identified cluster  $P_{1,1}, \dots, P_{1,6}$  to investigate the spectral homogeneity and further explore the possible presence of multiple changes in the re-projection in ASCVR scattergram. Reference vectors  $\mathbf{R}_{1,j}$  (i.e.,  $\alpha_{1,j}$ ,  $j=1, \dots, 6$ ) were automatically derived for each considered specific cluster, thus generating a 2-D representation for each of them. The corresponding six represented scattergrams  $\mathbf{D}_{1,1}-\mathbf{D}_{1,6}$  are illustrated in Fig.6 from (c) to (h). It is easy to see that four out of six clusters (i.e.,  $P_{1,1}$ ,  $P_{1,2}$ ,  $P_{1,5}$ ,  $P_{1,6}$ ) resulted in single homogenous classes in their corresponding representation domains (see Fig.6.c-d, g-h). These homogenous clusters were associated to different detected change classes. The two discriminable clusters observed in the representation of  $P_{1,3}$  and in  $P_{1,4}$  (i.e., Fig.6.e and f, respectively) were further analyzed and separated in the next level  $L_2$ , where both of them appeared as a single homogenous cluster on the corresponding ASCVR scattergram  $\mathbf{D}_{2,1}-\mathbf{D}_{2,4}$  (see Fig.6.i-l). Therefore, all eight change classes were successfully detected according to the proposed sequential analysis (four identified at level  $L_1$  and four at level  $L_2$ ).

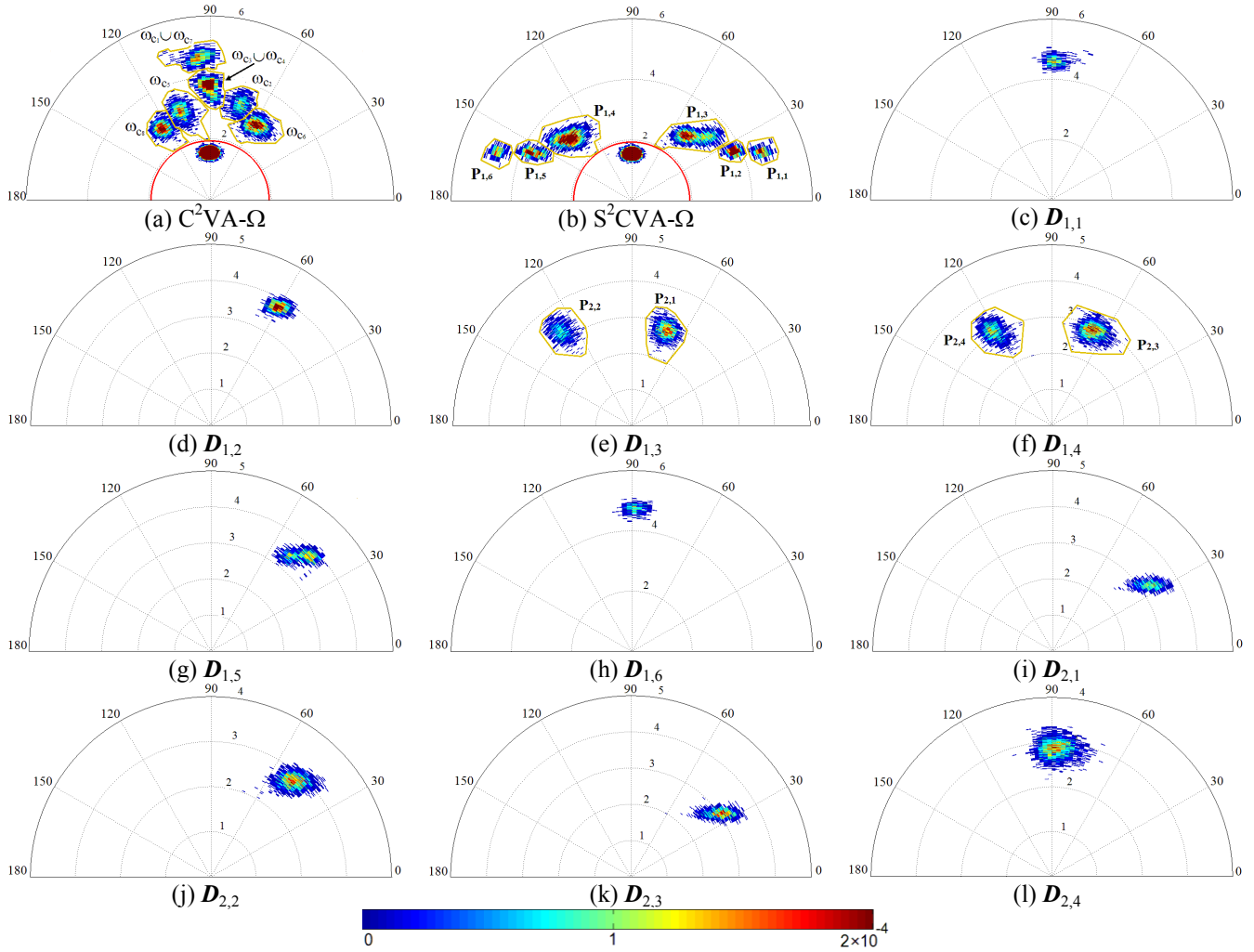


Fig.6 Change representation obtained by: (a)  $C^2VA\_M$ ; (b)-(l) proposed  $S^2CVA\_M$ . The sequence of ASCVR scattergrams represents changes at different levels of the  $S^2CVA$  hierarchy. Binary CD decision threshold is defined as red semicircle, whereas discrimination boundaries as yellow polygons. The final detected change classes are those obtaining a single homogenous cluster in their corresponding representation scattergrams (simulated hyperspectral remote sensing data set).

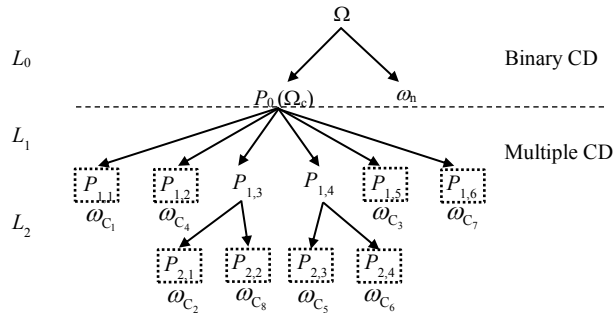


Fig.7 Three-level hierarchical tree obtained by the proposed  $S^2CVA\_M$  method. Nodes highlighted in dotted rectangles are the final detected changes (simulated hyperspectral remote sensing data set).

The obtained hierarchal tree of the considered CD-HS problem is shown in Fig.7. The correspondences among the identified clusters and the reference change classes are as follows:  $L_0: \Omega = \{\omega_n, \Omega_c(P_0)\}$ ;  $L_1: P_{1,1} = \omega_{C_1}$ ,  $P_{1,2} = \omega_{C_4}$ ,  $P_{1,3} = \{\omega_{C_2}, \omega_{C_8}\}$ ,  $P_{1,4} = \{\omega_{C_5}, \omega_{C_6}\}$ ,  $P_{1,5} = \omega_{C_3}$  and  $P_{1,6} = \omega_{C_7}$ ;  $L_2: P_{2,1} = \omega_{C_2}$ ,  $P_{2,2} = \omega_{C_8}$ ,  $P_{2,3} = \omega_{C_5}$  and  $P_{2,4} = \omega_{C_6}$ .

From the qualitative comparison of the change representation between the proposed  $S^2CVA\_M$  approach and the  $C^2VA\_M$  method, we can observe that:

- 1) The proposed ASCVR resulted in an improved change representation. Higher class separability among the change clusters can be found at the initial level of the representation (Fig.6.b) than in  $C^2VA$  one (Fig.6.a). The inter-class distances among change clusters are larger, thus making it easier to discover the clusters associated with different changes and to define the discrimination boundaries. On the contrary in the  $C^2VA$  the change clusters are more compressed and overlapped (see Fig.6.a). This confirms the usefulness of choosing the maximum eigenvector as the adaptive reference vector.
- 2) The proposed  $S^2CVA\_M$  method improves the change detectability. The hierarchical and adaptive scheme (i.e., use of adaptive reference vectors) for constructing spectral change variables allows one to discover and visualize more subtle spectral changes within the major change clusters detected at the first level  $L_1$  of the hierarchy. A fixed reference vector like in the  $C^2VA$  does not permit to investigate the latent spectral variations at different spectral detail levels, thus in most of the cases only the major changes are identified.
- 3) The proposed  $S^2CVA\_M$  results in a better change modeling. As discussed in Section III, the complexity of CD-HS problem reduces the effectiveness of the single level processing of  $C^2VA\_M$ . As shown in Fig.6 (a), the  $C^2VA$  representation does not distinguish some change classes. The proposed CD approach addresses the CD-HS problem by following a sequential fashion, thus it better considers the intrinsic hierarchical structure of changes in HS images.

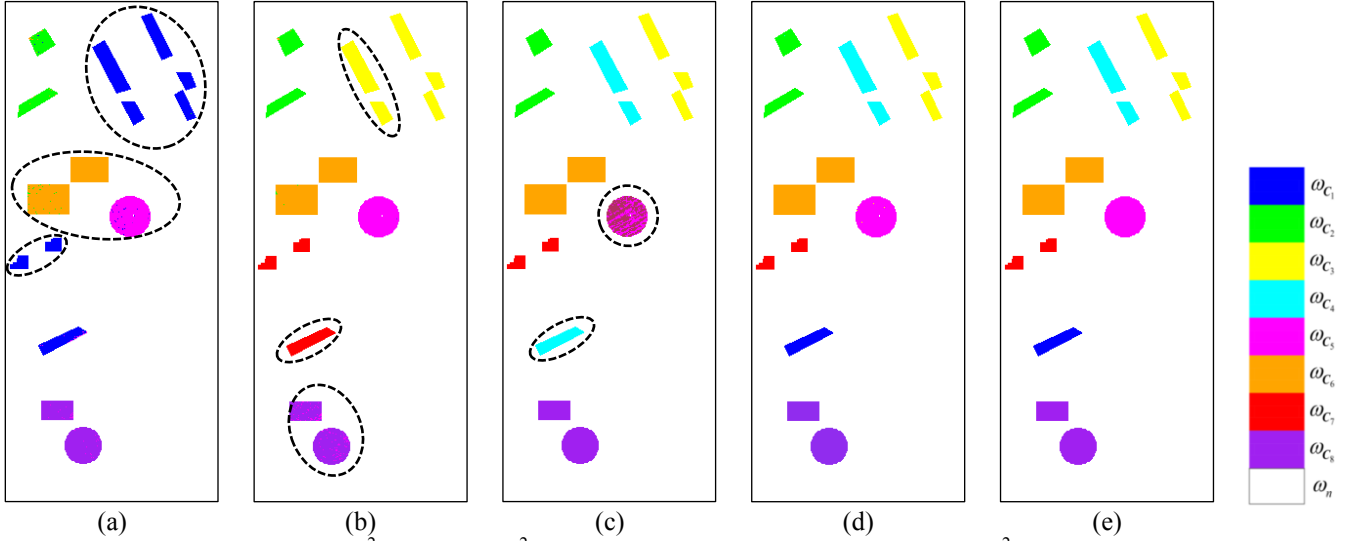


Fig.8 CD maps obtained by (a)  $C^2VA\_T$ ; (b)  $C^2VA\_M$ ; (c)  $k$ -means\_SCVs; (d) proposed  $S^2CVA\_M$ . (e) change reference map. Different changes are in different colors, and the no-change class is in white (simulated HS remote sensing data set).

**TABLE II**  
**NUMBER OF DETECTED KINDS OF CHANGE, DETECTION ACCURACY AND ERROR INDICES OBTAINED BY THE CONSIDERED METHODS (SIMULATED HYPERSPECTRAL REMOTE SENSING DATA SET).**

| CD Methods           | Number of detected kinds of change | OA (%) | Kappa  | Total errors (Number of pixels) |
|----------------------|------------------------------------|--------|--------|---------------------------------|
| $C^2VA\_T$           | 5                                  | -      | -      | -                               |
| $C^2VA\_M$           | 6                                  | -      | -      | -                               |
| $k$ -means_SCVs      | 8                                  | 98.77  | 0.9256 | 1371                            |
| Proposed $S^2CVA\_M$ | 8                                  | 99.99  | 0.9996 | 7                               |

The qualitative and quantitative comparisons of the CD results obtained by the other considered reference methods are shown in Fig.8 and TABLE II (where accuracy indices include the Overall Accuracy ( $OA$ ), Kappa Coefficient ( $Kappa$ ) and the number of mislabeled samples computed according to the available reference map), respectively. The qualitative analysis was conducted only on the methods resulting in the correct number of changes (i.e.,  $K=8$ ). The highlighted dotted circles in Fig.8 point out the main omission/commission errors occurred in each of the considered method. From the analysis of the quantitative CD results, we can observe that the  $C^2VA$ -based method did not detect all the changes due to the low class discriminability in the compressed change representation (see Fig.6.a). Only five and six changes were detected by using thresholding (i.e.,  $C^2VA\_T$ ) and interactive analysis (i.e.,  $C^2VA\_M$ ), respectively. Mixed changes and some false alarms are highlighted in Fig.8 (a) and (b).

Although the  $k$ -means\_SCVs was applied by providing as input the real number of changes (i.e.,  $K=8$ ), it resulted in a higher number of errors (i.e., 1371 pixels, mainly are commission errors, see Fig.8.c) than the proposed  $S^2CVA\_M$ . The proposed  $S^2CVA\_M$  approach achieved a very good CD result (see Fig.8.d, generated according to the sequence of scattergrams and the defined discrimination boundaries in Fig.6.b-l), resulting in the highest  $OA$  and  $Kappa$  values (i.e., 99.99% and 0.9996, respectively) with only 7 pixels of errors.

In addition, a detailed analysis of time taken from the proposed  $S^2CVA\_M$  approach has been conducted. In the experiments we used Matlab R2013a on an Intel i5-2400 quad-core 3.10 GHz PC with 4 GB of RAM. Time consumption has been evaluated considering the time required for: i) obtaining the initial binary change-detection step (only for the root node); ii) running the 2-D ASCVR; iii) identifying changes (here the time for manual cluster separation is provided by an estimation based on an average of multiple users' trials). In this data set, the proposed  $S^2CVA$  required in total 166.96 seconds (less than 3 minutes) to complete the hierarchy, where the binary CD step took 31.59 seconds and the user interaction required around 120 seconds. For each of the nodes, the processing time (i.e., sum of the ASCVR and change identification) is in the range of [0.9419, 2.0546] seconds. Therefore, the computation cost is very low.

### *B. Data Set 2: Simulated Hyperspectral Camera Data Set*

The second data set is related to a commercial HS camera (Nuance FX, CRI Inc.) image [30]. The image has 31 spectral bands with a spectral resolution of approximately 10 nm. The wavelength range is from 420nm to 720 nm, covering mainly the visible spectrum region. The considered image has a size of 1392  $\times$  1040 pixels. Based on the original image ( $X_1$ ), eight tiles were extracted over all the spectral bands and inserted into disjoint areas on a copy of  $X_1$ . Thus a synthetic image ( $X_2$ ) was generated, which includes ten change classes. A small constant bias value was applied to  $X_2$  and white Gaussian noise was added to

$X_2$  with an SNR value equal to 20dB. The false color composite of images  $X_1$  and  $X_2$  are shown in Fig. 9 (a) and (b), respectively. Fig. 9 (c) presents the change reference map. Note that changes were simulated considering either a material transitions or different illumination conditions for the same material. Thus subtle changes were introduced, and the complexity of the considered problem increased. More details the reader is referred to [23]. The same reference CD methods considered in the previous case were also applied to this data set.  $T_\rho$  for binary CD step was equal to 0.278. The  $C^2VA$  and  $S^2CVA$  representations are shown in Fig.10 (a) and (b)-(o), respectively, where the interactive change identification was done by the defined boundaries (see Fig.10). In this case the reference change map is also available due to the simulation procedure, so a fully quantitative evaluation was done by comparing the results obtained by the considered CD methods as in the previous experiment. The numeric results are shown in TABLE III.

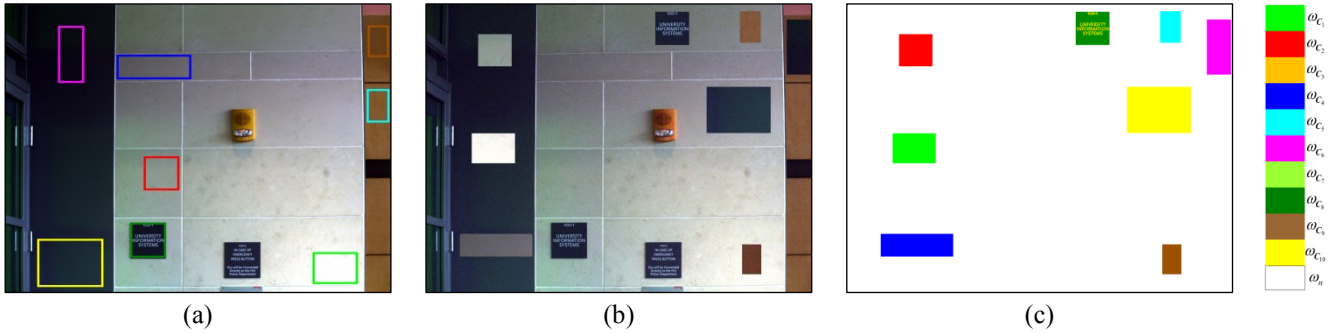


Fig. 9 False color composite (R: 710 nm; G: 620 nm; B: 510 nm) of (a) the HS image acquired by the Nuance FX HS camera ( $X_1$ ) and (b) simulated image with changes ( $X_2$ ). (c) Change reference map (ten changes in different colors, no-change class in white color).

**TABLE III**  
**NUMBER OF DETECTED KINDS OF CHANGE, DETECTION ACCURACY AND ERROR INDICES OBTAINED BY THE CONSIDERED METHODS (SIMULATED HYPERSPECTRAL CAMERA DATA SET).**

| CD Methods      | Number of detected kinds of change | OA (%) | Kappa  | Total errors (number of pixels) |
|-----------------|------------------------------------|--------|--------|---------------------------------|
| $C^2VA\_T$      | 4                                  | -      | -      | -                               |
| $C^2VA\_M$      | 7                                  | -      | -      | -                               |
| $k$ -means SCVs | 10                                 | 98.09  | 0.8949 | 12791                           |
| $S^2CVA\_M$     | 10                                 | 99.94  | 0.9964 | 801                             |

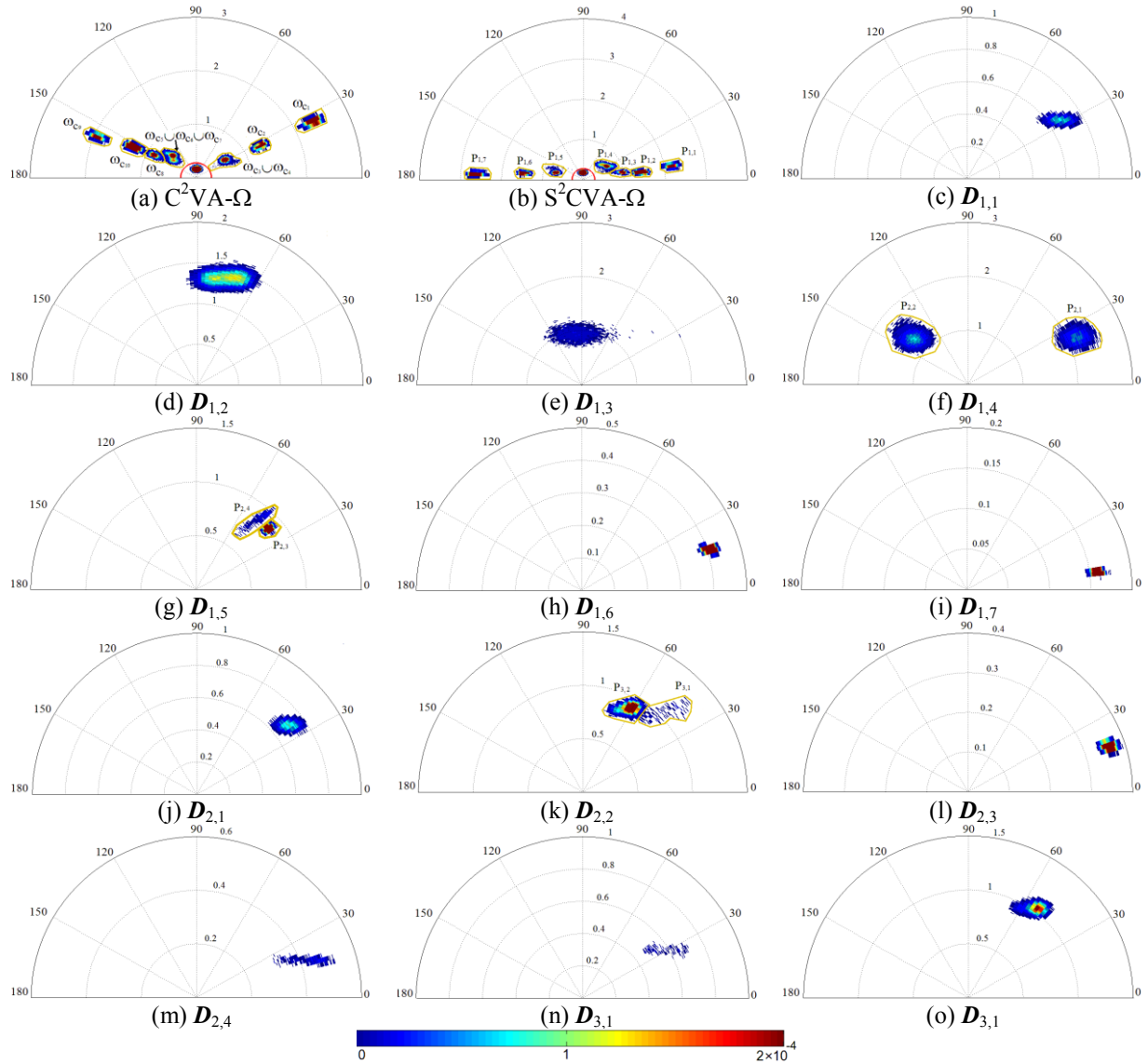


Fig.10 Change representation obtained by: (a) the  $C^2VA\_M$ ; (b)-(o) the proposed  $S^2CVA\_M$ . The sequence of ASCVR scattergrams represents changes at different levels of the  $S^2CVA$  hierarchy. Binary CD decision threshold is defined as red semicircle, whereas discrimination boundaries as yellow polygons. The final detected change classes are those obtaining a single homogenous cluster in their corresponding representation scattergrams (simulated hyperspectral camera data set).

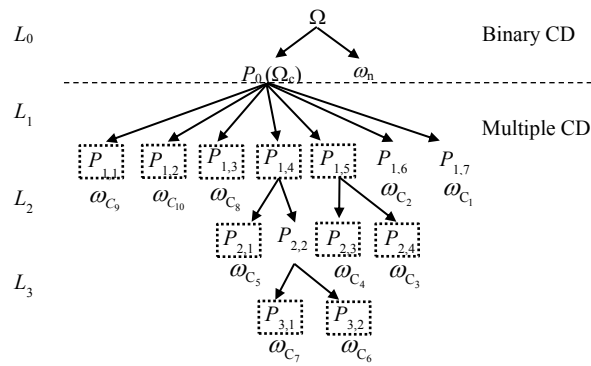


Fig.11 Four-level hierarchical tree obtained by the proposed  $S^2CVA\_M$  method. The nodes highlighted in dotted rectangles are the final detected changes (simulated hyperspectral camera data set).

From the results in TABLE III, we can observe that:

1) The  $C^2VA\_M$  separated and detected more changes (i.e.,  $K=7$ ) than the  $C^2VA\_T$  (i.e.,  $K=4$ ). However, both of them recognized less changes than the correct one (i.e.,  $K=10$ ) due to the poor change representation in  $C^2VA$  using the fixed unit reference vector.

2) The proposed  $S^2CVA\_M$  detected correctly all the ten changes, and achieved the highest  $OA$  (i.e., 99.94%) and  $Kappa$  (i.e., 0.9964). In this case the top-down procedure resulted in the four-level hierarchical tree as shown in Fig.11. Moreover, a fast and simple change identification was done interactively by using the proposed  $S^2CVA\_M$  approach.

3) The proposed  $S^2CVA\_M$  modeled better the hierarchical nature of the changes in HS images thus reduced the detection errors. Note that also in this case the  $k$ -means\_SCVs method was not able to correctly detect all changes even if it received as input the correct number of changes (i.e.,  $K=10$ ).

The same computation-cost evaluation was conducted as for the previous data set. The proposed  $S^2CVA\_M$  took 437.13 seconds (less than 8 minutes), where the binary step and manual interaction required 317.13 and 120 seconds, respectively. For each node, the processing cost is in the range of [4.72, 11.62] seconds. Thus, despite this data set has a large size (i.e.,  $1392 \times 1040 \times 31$ ), the proposed  $S^2CVA\_M$  still resulted in a low computation cost.

### *C. Data Set 3: Real Hyperion Remote Sensing Satellite Data Set*

The third data set is made up of a pair of real bi-temporal hyperspectral remote sensing images acquired by the Hyperion sensor mounted onboard the EO-1 satellite on May 1, 2004 ( $X_1$ ) and May 8, 2007 ( $X_2$ ), respectively. Images were downloaded from the U.S. Geological Survey (USGS) website [31]. The study area is an agricultural land of Hermiston city in Umatilla County, Oregon, United States. The selected area, which has a size of  $211 \times 396$  pixels, is a subset of the original whole image. The original images contain 242 spectral channels, whose wavelength range is from 350nm to 2580nm. The images

are characterized by a spectral resolution of 10nm and a spatial resolution of 30m. After the pre-processing phase (e.g., uncalibrated and noisiest bands removal, bad stripes repairing, atmospheric corrections, co-registration, etc.), 159 pre-processed bands (i.e., bands: 8-57, 82-119, 131-164, 182-184, 187-220) were used for testing the proposed CD approach. For more details on the data set and the pre-processing operations readers are referred to [23]. Fig.12 (a) and (b) show a false color composite of the two images. The changes occurred in the considered images include land-cover transitions between crops, bare soil, water, variations in soil moisture and in the water content of vegetation. For example, the circular fields (see Fig.12) change their spectral signatures mainly due to the effect of the agricultural irrigation system. In this case no ground truth data are available. Thus validation of the results was done in a qualitative way by a detailed visual comparison. Fig.12 (c) presents a false color composition of  $X_D$  by using three selected channels. Different colors represent the possible kinds of changes, whereas the gray areas indicate the unchanged pixels. In this work we are interested in detecting all kinds of changes affecting the spectral signatures. Note that the false color composition only shows the presence of changes in the considered wavelengths (i.e., R: 1729.70nm, G: 1023.40nm, B: 752.43nm). Changes that do not affect these wavelengths are not visible in Fig.12.

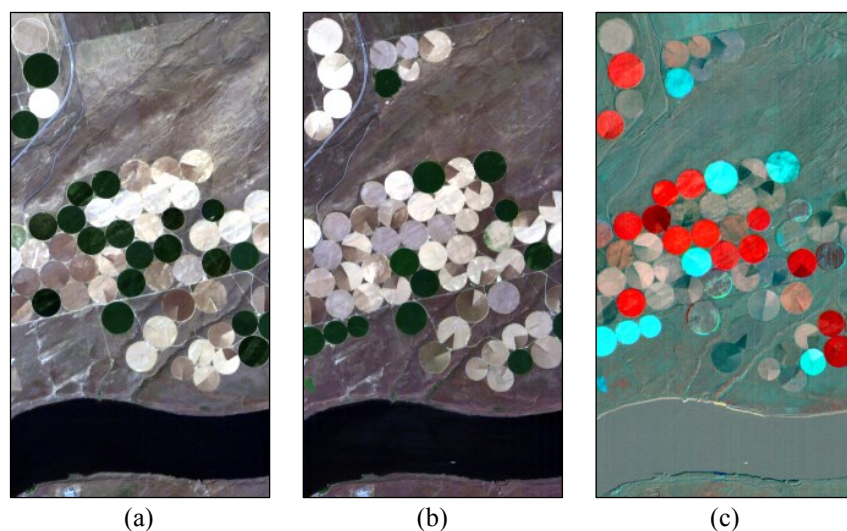


Fig.12 Real bi-temporal Hyperion images acquired on an agricultural scenario. False color composite (wavelength: R: 650.67nm, G: 548.92nm, B: 447.17nm) of the images acquired in (a) 2004 ( $X_1$ ) and (b) 2007 ( $X_2$ ). (c) Composite of three SCV channels (R: 1729.70nm, G: 1023.40nm, B: 752.43nm).

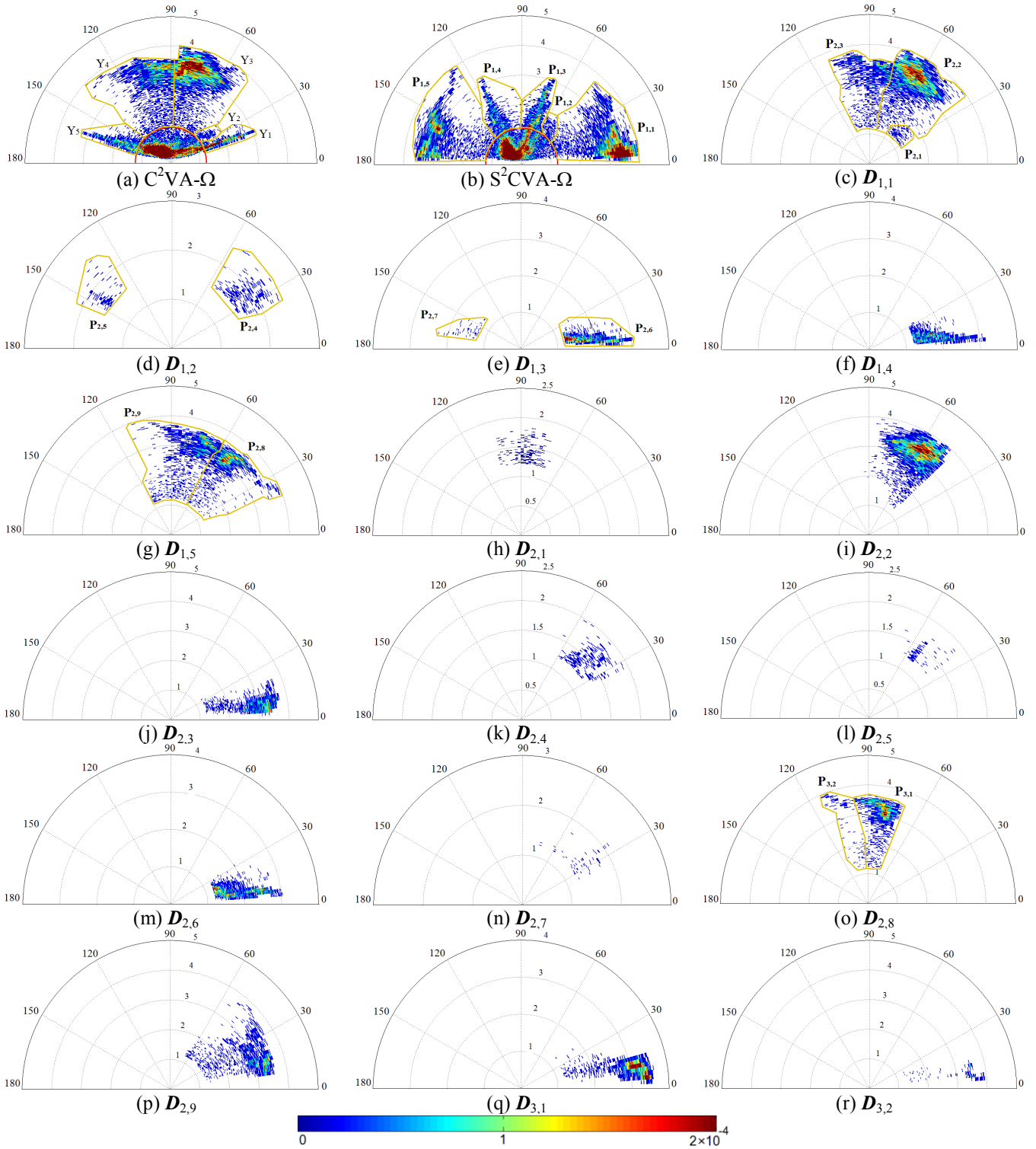


Fig.13 Change representations obtained by: (a)  $C^2VA\_M$ ; (b)-(r) the proposed  $S^2CVA\_M$  approach. A sequence of ASCVR scattergrams represents changes at different levels of the  $S^2CVA$  hierarchy. Binary CD threshold (i.e.,  $T_\rho$ ) is defined as red semicircle, whereas discrimination boundaries are defined as yellow polygons. The final detected change classes are those obtaining single homogenous cluster in their corresponding scattergrams (real HS Hyperion remote sensing data set).

Both the standard  $C^2VA$  and the proposed  $S^2CVA$  methods were applied to the considered images. The representation obtained by the  $C^2VA$  is shown in Fig.13 (a). The binary CD step was conducted on the magnitude  $\rho$  computed from all 159 spectral channels. The threshold  $T_\rho$  for separating the  $\Omega_c$  and  $\omega_n$  was estimated automatically [8] and was equal to 1.219 (see Fig.13.a, where  $T_\rho$  is represented as a red semicircle). Change identification was conducted, where the boundaries were interactively defined as yellow polygons. Five different change classes (see Fig.13.a) were detected. For the  $S^2CVA$ , the whole change structure and the sequence of ASCVR scattergrams obtained are illustrated in Fig.13 from (b) to (r), where each figure corresponds to a specific change cluster that is represented in a given level of the  $S^2CVA$  hierarchy. In the initial level of the sequential analysis (i.e.,  $L_0$ ), the binary CD step was performed as in the  $C^2VA$  (see Fig.13.b). Then the SCVs of the  $\Omega_c$  class ( $P_0$ ) were analyzed to discover other change classes and discrimination boundaries were defined for each of the scattering cluster in the representation domain (see Fig.13.b,  $D_{1,1}-D_{1,5}$ ). The  $S^2CVA$  process iterated until convergence was reached in each level of the hierarchy. Eleven kinds of change were detected by using the proposed  $S^2CVA$  method. The hierarchical tree is described in Fig.14. The obtained tree has four levels with nineteen nodes. Eleven of them correspond to the detected change classes and one to the no-change class. By analyzing the results shown in Fig.13 and Fig.14, we can observe that:

- 1) The  $C^2VA$  representation (i.e., Fig.13.a) results in changes that are overlapped to each other and their discrimination is almost impossible. A smaller number of change classes is identified by  $C^2VA\_M$  (i.e.,  $K=5$ , see Fig.13.a, cluster  $Y_1-Y_5$ ) than by the proposed  $S^2CVA\_M$  approach (i.e.,  $K=11$ ).
- 2) The proposed  $S^2CVA\_M$  method successfully addressed the considered CD-HS problem by decomposing it into several sub-problems. The multiple-change information was modeled and represented through seventeen ASCVR scattergrams. The sequence is automatically defined by investigating the inner-cluster spectral homogeneity at different levels. Note that changes merged in low

level representations become visible and separable in higher levels, thus allowing us to detect different kinds of changes in a hierarchical way, whose structure is described by the hierarchy tree in Fig.14.

3) The proposed unsupervised ASCVR approach properly discovers and represents changes by taking advantages of the specific SCVs for defining the reference vectors thus for computing the change variables. For each considered change cluster at a given level, the homogeneity is evaluated according to the represented 2-D scattergram, where a pure change results in a single homogenous scattering cluster. For example,  $\mathbf{D}_{1,3}$  represents two discriminable clusters in cluster  $P_{1,3}$ , whereas  $\mathbf{D}_{1,4}$  represents only one cluster in  $P_{1,4}$ , which indicates a higher homogeneity of the latter.

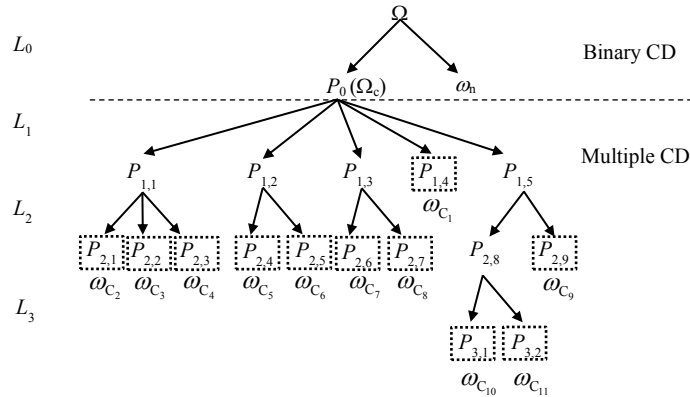


Fig.14 Four-level hierarchical tree obtained by proposed  $S^2CVA\_M$  method. Eleven change classes were identified and highlighted in dotted rectangles (real Hyperion remote sensing data set).

It is worth noting that the proposed method allows users to control the detection level, which is a very flexible property in real applications. If the aim is to identify more detailed subtle-change information, the process can go deeper down the hierarchy (i.e., detection of subtle changes that have slightly different realizations on their SCVs from the spectral behaviors of an associated change in the previous level [23]). In the proposed  $S^2CVA$  hierarchy, a change class is detected when it is associated with one homogenous cluster in its ASCVR representation (e.g., Fig.13.f, h-n, p-r). Sometime small changes (e.g., less than 10 pixels) might be discovered in the representation. For example, in Fig.13 (k), (n), (p) there are some SCVs that are isolated from the main (larger) change clusters. These kinds of clusters can be

relevant to some applications whereas they can be irrelevant to others. Thus the user can decide to stop the analysis at higher levels in the hierarchy where those changes are not separated yet. In our experiments, we followed this strategy and did not separate them.

The final CD maps generated by the proposed  $S^2CVA\_M$  and the considered reference methods are shown in Fig.15 (a)-(d). Different change classes appear in different colors and the no-change class is in white. The number of the detected changes in each method is listed in TABLE IV. Note that also in this case advantages were given to  $k$ -means\_SCVs method providing as input the number of changes (i.e.,  $K=11$ ) obtained by the proposed  $S^2CVA\_M$ . The performances of the considered methods were analyzed in a qualitative way by a detailed visual comparison.

**TABLE IV**  
**NUMBER OF DETECTED KINDS OF CHANGE IN THE CONSIDERED METHODS (REAL HYPERION**  
**REMOTE SENSING DATA SET).**

| CD Methods      | Number of detected kinds of change |
|-----------------|------------------------------------|
| $C^2VA\_T$      | 5                                  |
| $C^2VA\_M$      | 5                                  |
| $k$ -means_SCVs | 11                                 |
| $S^2CVA\_M$     | 11                                 |

As we can see from Fig.15 and TABLE IV, the two  $C^2VA$ -based methods (i.e.,  $C^2VA\_T$  and  $C^2VA\_M$ ) resulted in a small number of changes (i.e.,  $K=5$ ), which correspond to the major change classes. These changes show significant differences in spectral signatures in the SCV domain. However, many subtle changes are not visible and thus not detectable due to the compressed representation in  $C^2VA$  by using a fixed unit reference vector. The  $C^2VA\_M$  considered better the distribution of changes (Fig.13.a) thus resulting in a more reliable CD output than the  $C^2VA\_T$  (see Fig.15.b than Fig.15.a). By using the iterative analysis of the proposed  $S^2CVA$  method, more subtle changes became visible and detectable (see Fig.15.f) according to a systematic top-down procedure. These subtle change classes were not detectable by the  $C^2VA$ -based methods (see Fig.15.a-b).

The two  $C^2VA$ -based approaches detected fewer changes than the  $S^2CVA\_M$ . Some latent changes are still mixed in some detected clusters, which cannot be discriminated and separated by using  $C^2VA$  (see Fig.15.a and b). The  $S^2CVA\_M$  provided more convincing results than the  $k$ -means\_SCVs. This can be observed in Fig.15.d, where more homogenous change classes are present in the change-detection map. On the contrary, the  $k$ -means\_SCVs resulted in more fragments in the detected changes (see Fig.15.c). It is worth noting that the complex structure of the problem makes the use of clustering (which solves an ill-posed problem) less reliable than that of a user-manual decision. In the  $S^2CVA\_M$  users can control the decomposition into different levels, and the whole change representation and identification process. From the computation-cost point of view, the proposed  $S^2CVA\_M$  resulted in a very fast and efficient implementation. In this data set,  $S^2CVA\_M$  took in total 177.99 seconds (less than 3 minutes) to evaluate the four-level hierarchy for the change discovery, representation and detection. In greater details, the binary CD step took 24.80 seconds, and the user interaction required around 120 seconds.

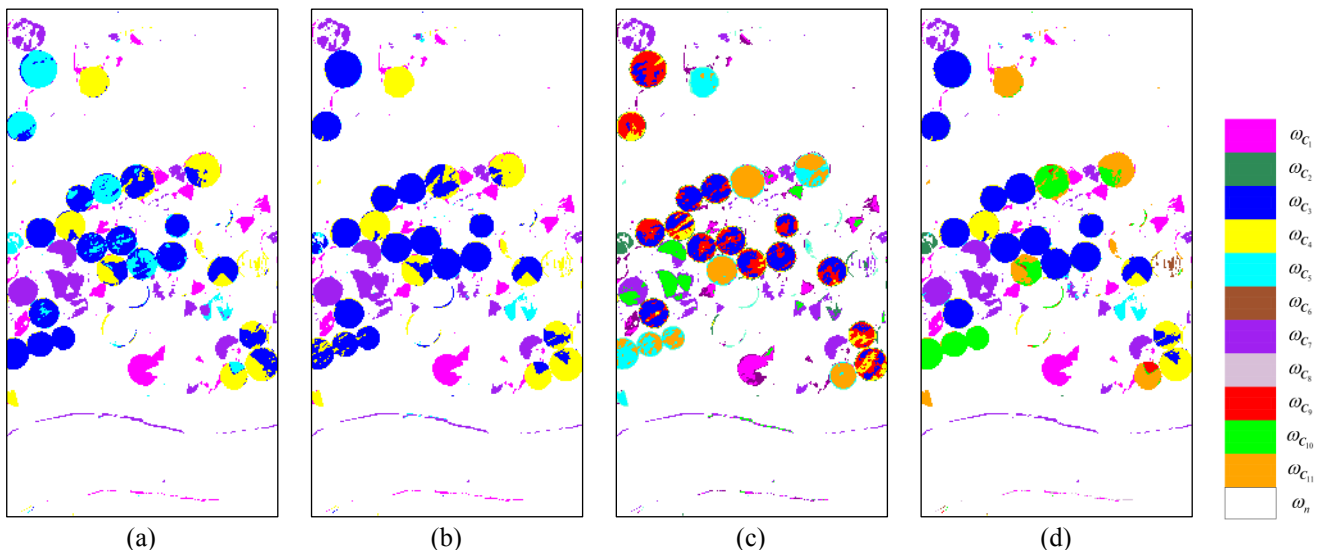


Fig.15 Change-detection maps obtained by (a)  $C^2VA\_T$ ; (b)  $C^2VA\_M$ ; (c)  $k$ -means\_SCVs; (d)  $S^2CVA\_M$  (according to the discrimination boundaries defined in Fig.13. (b)-(e), (g) and (o)). Different changes are in different colors, and the no-change class is in white color (real HS Hyperion remote sensing data set).

## V. DISCUSSION AND CONCLUSION

In this paper, a novel sequential spectral change vector analysis ( $S^2CVA$ ) approach has been proposed in order to address the challenging multiple-change detection problem in multitemporal HS images. Developed on the basis of the  $C^2VA$  state-of-the-art method, the proposed approach aims at discovering, representing and detecting multiple changes according to a sequential process that takes into account different levels of spectral change significance. The main novelties of the proposed  $S^2CVA$  are: 1) It iteratively analyzes the heterogeneous change information by following a top-down structure and a sequential analysis. Thus changes can be represented, discovered and detected at different levels of the hierarchy. 2) At each level it adaptively exploits the proposed ASCVR to represent changes by using a reference vector automatically and adaptively defined. Experimental results obtained on both simulated and real multitemporal HS images confirmed the effectiveness of the proposed approach.

Based on the theoretical analysis and the empirical experimental results we can also conclude that:

- 1) The proposed  $S^2CVA$  method extends the use of  $C^2VA$  to HS images where a large number of major and subtle changes may be present in the high dimensional data. Changes are discovered and separated according to their intrinsic spectral behaviors in SCVs, which are represented by a hierarchical tree. The computational complexity of the proposed  $S^2CVA$  method is very low (in all our experiments few minutes were required for the entire processing on a standard PC). It is worth noting that, despite the total processing time depends on the hierarchical tree size, any additional node requires in average few seconds. Thus the iterative nature on the process does not represent a critical limitation in real applications. Note that the proposed method can also be used for addressing the CD-MS problem. In this case we expect that the hierarchy results in fewer levels.
- 2) Unlike the standard  $C^2VA$ , the proposed ASCVR method adaptively and automatically changes the reference vectors according to the SCVs of the specific changes that are analyzed. Therefore, although the compression from the  $B-D$  to the 2-D feature space introduces an unavoidable loss of information,

the sequential analysis gradually recovers in the hierarchy the information loss at first levels, resulting in complete change representations and in satisfactory change-detection maps.

3) The proposed change identification approach allows us to directly extract the change information in the ASCVR domain of interest of the user, thus providing an easy but efficient way to address the change discovery and separation problem in complex problems with HS images.

An apparent limitation of the proposed method is that it results in a semi-automatic implementation (changes are detected via interaction with the user), which does not allow a completely automatic detection of changes. However, we would like to point out that the main goal of the proposed approach is to have an effective top-down procedure that supports the user in discovering and analyzing changes through an interactive process. This is very important for addressing CD problems with HS images.

Future developments of this work will be focused on: 1) study of other change representation variables aimed to further enhance the change representation; and 2) joint use of the spatial-spectral multiresolution information to reduce the misregistration effect.

#### ACKNOWLEDGEMENTS

This work was carried out in the framework of the project “Very high spatial and spectral resolution remote sensing: a novel integrated data analysis system”, funded by the Italian Ministry of Education, University and Research (Ministero dell'Istruzione, dell'Università e della Ricerca - MIUR) as a research program of relevant national interest (Programmi di Ricerca di Rilevante Interesse Nazionale – PRIN 2012). This work was also partially supported by the National Key Scientific Instrument and Equipment Development Project (No. 012YQ050250) and the Jiangsu Provincial Natural Science Foundation (No. BK2012018).

#### REFERENCES

- [1] L. Bruzzone and F. Bovolo, "A Novel Framework for the Design of Change-Detection Systems for Very-High-Resolution Remote Sensing Images," *Proceedings of the IEEE*, vol. 101, no. 3, pp. 609 - 630, 2013.
- [2] A. Singh, "Digital change detection techniques using remotely-sensed data," *International Journal of Remote Sensing*, vol. 10, no. 6, pp. 989-1003, 1989.
- [3] P. Coppin, I. Jonckheere, K. Nackaerts, B. Muys and E. Lambin, "Digital change detection methods in

- ecosystem monitoring: a review," *International Journal of Remote Sensing* , vol. 25, no. 9, pp. 1565-1596, 2004.
- [4] D. Lu, P. Mause, E. Brondízio and E. Moran, "Change detection techniques," *International Journal of Remote Sensing* , vol. 25, no. 12, pp. 2365-2401, 2004.
- [5] P. R. Coppin and M. E. Bauer, "Digital change detection in forest ecosystems with remote sensing imagery," *Remote Sensing Reviews*, vol. 13, no. 3-4, pp. 207-304, 1996.
- [6] M. K. Ridd and J. Liu, "A Comparison of Four Algorithms for Change Detection in an Urban Environment," *Remote Sensing of Environment*, vol. 63, no. 2, pp. 95-100, 1998.
- [7] L. Bruzzone and D. F. Prieto, "A minimum-cost thresholding technique for unsupervised change detection," *International Journal of Remote Sensing*, vol. 21, no. 18, pp. 3539-3544, 2000.
- [8] L. Bruzzone and D. Prieto, "Automatic analysis of the difference image for unsupervised change detection," *Geoscience and Remote Sensing, IEEE Transactions on* , vol. 38, no. 3, pp. 1170-1182, 2000.
- [9] T. Celik, "Unsupervised Change Detection in Satellite Images Using Principal Component Analysis and k-Means Clustering," *Geoscience and Remote Sensing Letters, IEEE* , vol. 6, no. 4, pp. 772-776, 2009.
- [10] S. L. Hégarat-Mascle and R. Seltz, "Automatic change detection by evidential fusion of change indices," *Remote Sensing of Environment*, vol. 91, no. 3-4, pp. 390-404, 2004.
- [11] P. Du, S. Liu, P. Gamba, K. Tan and J. Xia, "Fusion of Difference Images for Change Detection over Urban Areas," *Selected Topics in Applied Earth Observations and Remote Sensing, IEEE Journal of*, vol. 5, no. 4, pp. 1076-1086, 2012.
- [12] P. Du, S. Liu, J. Xia and Y. Zhao, "Information fusion techniques for change detection from multi-temporal remote sensing images," *Information Fusion*, vol. 14, no. 1, pp. 19-27, 2013.
- [13] V. Soares and R. Hoffer, "Eucalyptus forest change classification using multi-data Landsat TM data," in *Proceedings, SPIE*, 1994.
- [14] L. Bruzzone and S. Serpico, "An iterative technique for the detection of land-cover transitions in multitemporal remote-sensing images," *Geoscience and Remote Sensing, IEEE Transactions on*, vol. 35, no. 4, pp. 858-867, 1997.
- [15] B. Demir, F. Bovolo and L. Bruzzone, "Detection of Land-Cover Transitions in Multitemporal Remote Sensing Images With Active-Learning-Based Compound Classification," *Geoscience and Remote Sensing, IEEE Transactions on*, vol. 50, no. 5, pp. 1930 - 1941, 2012.
- [16] A. Nielsen, "The Regularized Iteratively Reweighted MAD Method for Change Detection in Multi- and Hyperspectral Data," *IEEE Trans. on Image Proc.*, vol. 16, no. 2, pp. 463-478, 2007.
- [17] V. Ortiz-Rivera, M. Vélez-Reyes and B. Roysam, "Change detection in hyperspectral imagery using temporal principal components," in *Proc. SPIE 6233, Algorithms and Technologies for Multispectral, Hyperspectral, and Ultraspectral Imagery XII*, Orlando (Kissimmee), FL, 2006.
- [18] F. Bovolo, S. Marchesi and L. Bruzzone, "A Framework for Automatic and Unsupervised Detection of Multiple Changes in Multitemporal Images," *Geoscience and Remote Sensing, IEEE Transactions on*, vol. 50, no. 6, pp. 2196-2212, 2012.
- [19] W. A. Malila, "Change Vector Analysis: An Approach for. Detecting Forest Changes with Landsat," in *6th Annual Symposium on Machine Processing of Remotely Sensed Data*, West Lafayette, Indiana, 1980.
- [20] F. Bovolo and L. Bruzzone, "A Theoretical Framework for Unsupervised Change Detection Based on Change Vector Analysis in the Polar Domain," *Geoscience and Remote Sensing, IEEE Transactions on*, vol. 45, no. 1, pp. 218-236, 2007.
- [21] F. Bovolo and L. Bruzzone, "An adaptive thresholding approach to multiple-change detection in multispectral images," in *Geoscience and Remote Sensing Symposium (IGARSS), 2011 IEEE International*, Vancouver, BC, 2011.
- [22] C.-I. Chang, *Hyperspectral Imaging: Techniques for Spectral Detection and Classification*, New York:

Plenum Publishing Co., 2003.

- [23] S. Liu, L. Bruzzone, F. Bovolo and P. Du, "Hierarchical change detection in multitemporal hyperspectral images," *Geoscience and Remote Sensing, IEEE Transactions on*, vol. 53, no. 1, pp. 244 - 260 , 2015.
- [24] N. Keshava, "Distance Metrics and Band Selection in Hyperspectral Processing With Applications to Material Identification and Spectral Libraries," *Geoscience and Remote Sensing, IEEE Transactions on*, vol. 42, no. 7, pp. 1552-1565, 2004.
- [25] C. Chang, "An information-theoretic approach to spectral variability, similarity, and discrimination for hyperspectral image," *IEEE Transactions on Information Theory*, vol. 46, no. 5, pp. 1927-1932, 2000.
- [26] Y. Sohn and N. S. Rebello, "Supervised and unsupervised spectral angle classifiers," *Photogrammetric Engineering and Remote Sensing*, vol. 68, no. 12, pp. 1271-1280, 2002.
- [27] P. Du, S. Liu, L. Bruzzone and F. Bovolo, "Target-driven change detection based on data transformation and similarity measures," in *2012 IEEE International Geoscience and Remote Sensing Symposium*, Munich, Germany, 2012.
- [28] A. Ghosh, N. S. Mishra and S. Ghosh, "Fuzzy clustering algorithms for unsupervised change detection in remote sensing images," *Information Sciences*, vol. 181, no. 4, pp. 699-715 , 2011.
- [29] [Online]. Available: [http://www.ehu.es/ccwintco/index.php/Hyperspectral\\_Remote\\_Sensing\\_Scenes](http://www.ehu.es/ccwintco/index.php/Hyperspectral_Remote_Sensing_Scenes).
- [30] A. Chakrabarti and T. Zickler, "Statistics of Real-World Hyperspectral Images," in *in Proceedings of the IEEE Conference on Computer Vision and Pattern Recognition (CVPR)*, 2011.
- [31] [Online]. Available: <http://earthexplorer.usgs.gov/>.



**Sicong Liu** received the B.Sc. degree in Geographical Information System and the M.E. degree in photogrammetry and remote sensing from China University of Mining and Technology, Xuzhou, China, in 2009 and 2011, respectively. He is currently a Ph.D. student with the Remote Sensing Laboratory, Department of Information Engineering and Computer Science, University of Trento, Italy. His research interests include multitemporal data analysis, change detection, spectral signal analysis in multispectral /hyperspectral images.

He serves as a reviewer for several international remote sensing journals, including *IEEE Transactions on Geoscience and Remote Sensing*, *IEEE Journal of Selected Topics in Applied Earth Observations and Remote Sensing*, *IEEE Geoscience and Remote Sensing Letters*, *ISPRS Journal of Photogrammetry and Remote Sensing*, *Remote Sensing*, etc.



**Lorenzo Bruzzone** (S'95–M'98–SM'03–F'10) received the Laurea (M.S.) degree in electronic engineering (summa cum laude) and the Ph.D. degree in telecommunications from the University of Genoa, Italy, in 1993 and 1998, respectively.

He is currently a Full Professor of telecommunications at the University of Trento, Italy, where he teaches remote sensing, radar, pattern recognition, and electrical communications. Dr. Bruzzone is the founder and the director of the Remote Sensing Laboratory in the Department of Information Engineering and Computer Science, University of Trento. His current research interests are in the areas of remote sensing, radar and SAR, signal processing, and pattern recognition. He promotes and supervises research on these topics within the frameworks of many national and international projects. Among the others, he is the Principal Investigator of the *Radar for icy Moon exploration (RIME)* instrument in the framework of the *Jupiter ICy moons Explorer (JUICE)* mission of the European Space Agency. He is the author (or coauthor) of 150 scientific publications in referred international journals (101 in IEEE journals), more

than 215 papers in conference proceedings, and 16 book chapters. He is editor/co-editor of 11 books/conference proceedings and 1 scientific book. His papers are highly cited, as proven from the total number of citations (more than 9620) and the value of the h-index (51) (source: Google Scholar). He was invited as keynote speaker in 24 international conferences and workshops. Since 2009 he is a member of the Administrative Committee of the IEEE Geoscience and Remote Sensing Society.

Dr. Bruzzone ranked first place in the Student Prize Paper Competition of the 1998 IEEE International Geoscience and Remote Sensing Symposium (Seattle, July 1998). Since that time he was recipient of many international and national honors and awards. Dr. Bruzzone was a Guest Co-Editor of different Special Issues of international journals. He is the co-founder of the IEEE International Workshop on the Analysis of Multi-Temporal Remote-Sensing Images (MultiTemp) series and is currently a member of the Permanent Steering Committee of this series of workshops. Since 2003 he has been the Chair of the SPIE Conference on Image and Signal Processing for Remote Sensing. Since 2013 he has been the founder Editor-in-Chief of the IEEE GEOSCIENCE AND REMOTE SENSING MAGAZINE. Currently he is an Associate Editor for the IEEE TRANSACTIONS ON GEOSCIENCE AND REMOTE SENSING and the CANADIAN JOURNAL OF REMOTE SENSING. Since 2012 he has been appointed *Distinguished Speaker* of the IEEE Geoscience and Remote Sensing Society.



**Francesca Bovolo** (S'05–M'07–SM'13) received the “Laurea” (B.S.), the “Laurea Specialistica” (M.S.) degrees in telecommunication engineering (*summa cum laude*) and the Ph.D. in Communication and Information Technologies from the University of Trento, Italy, in 2001, 2003 and 2006, respectively where she has been a research fellow until June 2013.

She is the founder and the head of the Remote Sensing for Digital Earth unit at Fondazione Bruno Kessler (FBK), Trento, Italy and a member of the Remote Sensing Laboratory (RSLab) in Trento.

Her main research activity is in the area of remote-sensing image processing. Her interests are related to multitemporal remote sensing image analysis, change detection in multispectral, hyperspectral and SAR images, and very high resolution images, content-based time series retrieval, and domain adaptation. She conducts research on these topics within the context of several national and international projects. She is a referee for several international journals. She is one of the Co-Investigatortors of the Radara for Icy Moon Exploration (RIME) instrument of the ESA JUPITER Icy moons Explorer (JUICE).

Dr. Bovolo ranked first place in the Student Prize Paper Competition of the 2006 *IEEE International Geoscience and Remote Sensing Symposium* (Denver, August 2006). Since January 2011 she is an associate editor of the *IEEE Journal of Selected Topics in Applied Earth Observations and Remote Sensing*. She has been guest editor for the Special Issue on “Analysis of Multitemporal Remote Sensing Data” of the *IEEE Transactions on Geoscience and Remote Sensing*. She is the Technical Chair of the Sixth International Workshop on the Analysis of Multi-temporal Remote-Sensing Images (MultiTemp 2011). From 2006 to 2013, she has served on the Scientific Committee of the SPIE International Conference on “Signal and Image Processing for Remote Sensing”. Since 2014 she is co-chair of the same conference. She is the publication chair for *International Geoscience and Remote Sensing Symposium 2015*. Since 2012 she is a member of the international program committee of the conference on *Pattern Recognition Applications and Methods*. She has served on the Scientific Committee of the *IEEE Fourth and Fifth International Workshop on the Analysis of Multi-Temporal Remote Sensing Images (MultiTemp 2007 and 2009)* and of the *IEEE GOLD Remote Sensing Conference* in 2010, 2012, and 2014.



**Massimo Zanetti** received the M.S. degree in Mathematics from the University of Ferrara, Italy. Currently, he is a Ph.D. Student with the Remote Sensing Laboratory at the Department of Information and Communication Technologies, University of Trento, Trento, Italy.

His research interests include change detection, multispectral images analysis, variational methods for segmentation, numerical optimization.



**Peijun Du** (M'07-SM'12) received the B.S. and Ph.D. degrees in Geomatics engineering and cartography and geographic information system from China University of Mining and Technology, Xuzhou, China, in 1997 and 2001, respectively. Currently, he is a Professor of photogrammetry and remote sensing at the Department of Geographical Information Science, Nanjing University, Nanjing, China.

From 2002 to 2004, he was a postdoctoral fellow with the Lab of Pattern Analysis & Machines Intelligence, Institute of Image Processing and Pattern Recognition, Shanghai Jiaotong University (SJTU), Shanghai, China. During 2006 to 2007, he was a visiting scholar at the University of Nottingham, Nottingham, U.K. His research interests include remote sensing image processing and pattern recognition, remote sensing applications, hyperspectral remote sensing information processing, multi-source geospatial information fusion and spatial data handling, integration and applications of geospatial information technologies, and environmental information science (environmental informatics). He is the author of nine books in Chinese and more than 100 research articles about remote sensing and geospatial information processing and applications.

Dr. Du was the Co-chair of the Technical Committee, URBAN 2009 (the 5th IEEE GRSS/ISPRS Joint Workshop on Remote Sensing and Data Fusion over Urban Areas), and the Co-chair of the local organizing committee of JURSE 2009. He also served as the member of scientific committee or local organizing committee of other international conferences, for example, Accuracy 2008, ACRS 2009, WHISPERS 2010, 2011 and 2012, URBAN 2011, MultiTemp 2011, and ISDIF 2011. He is a member of International Society of Environment Information Science and IEEE GRSS, and a council member of China Society for Image and Graphics (CSIG), China Association for Remote Sensing Applications (CARSA) and Jiangsu Provincial Society of Remote Sensing and Geographic Information System. He is also an Associate Editor for IEEE Geoscience and Remote Sensing Letters.